INT. J. NUM. METH. HEAT FLUID FLOW, VOL. 4, 553–559 (1994)

A NUMERICAL STUDY OF FREE CONVECTIVE HEAT TRANSFER IN A PARALLELOGRAM-SHAPED ENCLOSURE

D. NAYLOR

Department of Mechanical Engineering, Ryerson Polytechnic University, Toronto, Ont. M5B 2K3, Canada

AND

P. H. OOSTHUIZEN

Heat Transfer Laboratory, Department of Mechanical Engineering, Queen's University, Kingston, Ont. K7L 3N6, Canada

ABSTRACT

Two-dimensional free convective flow in a parallelogram-shaped enclosure has been studied numerically. The heated and cooled walls of the enclosure are isothermal and inclined at an angle β with respect to gravity. The top and bottom walls of the enclosure are horizontal and adiabatic. Calculations have been made for Rayleigh numbers ranging from 10^3 to 10^5 for a variety of wall angles ($-60° \leqslant \beta \leqslant 60°$) and enclosure aspect ratios $0.5 \leqslant A \leqslant 3$. Average and local Nusselt number results are presented for a Prandtl number of 0.7. Streamline and isotherm contours are also presented.

KEY WORDS Free convection Enclosure Parallelogram Finite element formulation

NOMENCLATURE

A	aspect ratio, H'/W',
k	thermal conductivity,
g	acceleration due to gravity,
h	local heat transfer coefficient,
H'	length of inclined walls of enclosure,
$\underline{Nu}$	local Nusselt number, hW'/k,
Nu	average Nusselt number,
n	unit normal vector,
Pr	Prandtl number,
q	local heat transfer rate,
Ra	Rayleigh number based on the enclosure width, $g\beta(T'_H - T'_C)W'^3/(\nu\alpha)$,
Ra^*	Rayleigh number based on the enclosure height, $g\beta(T'_H - T'_C)(H' \cos \beta)^3/(\nu\alpha)$,
T', T	temperature and dimensionless temperature,
T'_C	cold wall temperature,
T'_H	hot wall temperature,
u', v'	velocity components in the x' and y' directions,
W'	width of the enclosure,
x, y	dimensionless Cartesian coordinates,
x', y'	Cartesian coordinates,
y_p^*	coordinate along heated wall.

Greek

α	thermal diffusivity,
β	wall inclination angle from vertical,
ν	kinematic viscosity,
ψ', ψ	stream function and dimensionless stream function,
ω', ω	vorticity and dimensionless vorticity.

0961–5539/94/060553–07$2.00

Received May 1993
Revised December 1993

INTRODUCTION

Two-dimensional free convective flow in an enclosure with one wall heated and one wall cooled is an approximate model of many situations of practical interest. For this reason it has been studied extensively for rectangular-shaped enclosures. In comparison, free convection in non-rectangular geometries has received much less attention. In the present investigation, laminar free convective heat transfer in a parallelogram-shaped enclosure has been studied numerically. The model geometry is shown in *Figure 1*. The enclosure has an isothermal hot wall at temperature T'_H and an isothermal cold wall at temperature T'_C, both inclined at an angle β with respect to vertical. The horizontal walls are adiabatic.

Previous studies of free convection in parallelogram-shaped enclosures have been motivated primarily by applications to so-called 'one-way' heat walls. A 'one-way' heat wall is a hollow wall with internal partitions that form many stacked parallelogram-shaped enclosures. In this application the hot and cold walls are vertical and the adiabatic partitions are inclined so that the free convective motion (and heat transfer rate) is much greater when the hot side of each parallelogrammic chamber is lower than the cold side. For this configuration, there have been several numerical studies[1–3] and experimental studies[4,5] of two-dimensional free convection. Also, Yang *et al.*[6] have performed calculations for three-dimensional free convection in a parallelepiped enclosure with inclined adiabatic walls and vertical hot/cold walls. The effect of non-orthogonal walls on free convection in an enclosure has also been studied by Lee[7], who obtained numerical and experimental data for low aspect ratio inclined trapezoidal enclosures.

In contrast to the above-mentioned studies, the present study provides new information about effect of inclining the hot and cold surfaces on the free convective heat transfer rate in an parallelogram-shaped enclosure. One application of this work is to predict heat losses from complex shaped air spaces (such as across wall spaces). Also, the current geometry represents an approximate model of some electrical and electronics cooling applications.

GOVERNING EQUATIONS AND SOLUTION PROCEDURE

The flow is assumed to be steady, laminar, incompressible and two dimensional. Fluid properties are assumed to be constant, except for density which is treated by means of the Boussinesq approximation. The solution has been obtained in terms of the stream function (ψ') and vorticity (ω'), defined as:

$$u' = \frac{\partial \psi'}{\partial y'} \qquad v' = -\frac{\partial \psi'}{\partial x'} \tag{1}$$

$$\omega' = \frac{\partial v'}{\partial x'} - \frac{\partial u'}{\partial y'} \tag{2}$$

In terms of these variables, the governing equations become:

$$\frac{\partial^2 \psi}{\partial x^2} + \frac{\partial^2 \psi}{\partial y^2} = -\omega \tag{3}$$

$$\frac{\partial^2 \omega}{\partial x^2} + \frac{\partial^2 \omega}{\partial y^2} = \frac{1}{Pr}\left(\frac{\partial \psi}{\partial y}\frac{\partial \omega}{\partial x} - \frac{\partial \psi}{\partial x}\frac{\partial \omega}{\partial y}\right) - Ra\frac{\partial T}{\partial x} \tag{4}$$

$$\frac{\partial^2 T}{\partial x^2} + \frac{\partial^2 T}{\partial y^2} = \frac{\partial \psi}{\partial y}\frac{\partial T}{\partial x} - \frac{\partial \psi}{\partial x}\frac{\partial T}{\partial y} \tag{5}$$

where the following dimensionless variables have been defined:

$$x = x'/W' \qquad y = y'/W' \qquad T = (T' - T'_c)/(T'_H - T'_c) \tag{6}$$

$$\psi = \psi' Pr/\nu \qquad \omega = \omega' W'^2 Pr/\nu \tag{7}$$

and the Rayleigh number based on the enclosure width is:

$$Ra = g\beta(T'_H - T'_c)W'^3/\nu\alpha \tag{8}$$

Referring to *Figure 1*, the boundary conditions are:

$$\begin{aligned} &\textit{Adiabatic walls BC and AD:} && \psi = 0, \partial\psi/\partial y = 0, \partial T/\partial y = 0 \\ &\textit{Inclined hot wall AB:} && \psi = 0, \partial\psi/\partial n = 0, T = 1 \\ &\textit{Inclined cold wall DC:} && \psi = 0, \partial\psi/\partial n = 0, T = 0 \end{aligned} \tag{9}$$

where n is the unit normal vector.

The dimensionless equations have been solved subject to the above boundary conditions using a Galerkin finite element method. Triangular elements with linear interpolation functions were used. The solution procedure has been used successfully in a number of previous studies free convection in enclosures[8,9]. Also, to validate the solution procedure, calculations have been made for the case of a square enclosure ($A = H'/W' = 1$, $\beta = 0°$). As shown in *Table 1*, the average Nusselt number data from the present solution is in close agreement with the bench mark solution of De Vahl Davis and Jones[10]. Grid testing was performed for a range of parameters. For example, calculations were performed for 21×21, 31×31 and 41×41 non-uniform grids (for $A = 1.0$). At the highest Rayleigh number $Ra = 10^5$ (worst case), the average Nusselt number data were grid independent to within 2%.

The solution directly gives the local dimensionless heat transfer rate distributions on the hot and cold walls. The local Nusselt number has been defined as:

$$Nu = \frac{qW'}{k(T'_H - T'_c)} \tag{10}$$

where q is the local heat transfer rate and k is the thermal conductivity. These local Nusselt number distributions are integrated over each surface to yield the average Nusselt number ($\overline{Nu}$).

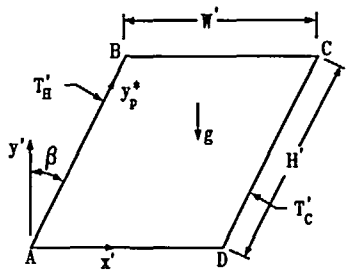

Figure 1 The model geometry

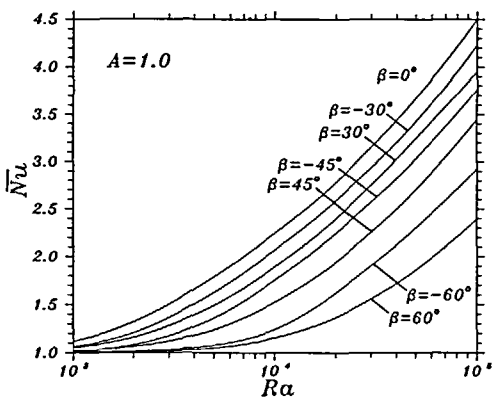

Figure 2 Variation of the average Nusselt number with Rayleigh number for wall angles $\beta = 0°$, $\pm 30°$, $\pm 45°$, $\pm 60°$ and for an aspect ratio $A = 1.0$

It should be noted that with this definition, the Nusselt number is not equal to the ratio of the mean heat transfer rate to the pure conduction heat transfer rate (except for cases with $\beta = 0°$, and cases with $A = 1.0$). However, this ratio can be easily deduced from the results presented. Note also that in *Figure 1*, a coordinate y_p^* along the hot wall has been defined for the purpose of presenting local Nusselt number data.

RESULTS

The solution to the governing equations given in the previous section has the following parameters:

- Rayleigh number, Ra
- Prandtl number, Pr
- Aspect ratio of the enclosure, $A = H'/W'$
- Hot and cold wall angle, β

The range of parameters considered in this study is, $10^3 \leqslant Ra \leqslant 10^5$, $0.5 \leqslant A \leqslant 3$, and $-60° \leqslant \beta \leqslant 60°$. Solutions have been obtained for only $Pr = 0.7$ because the most likely applications are for air.

Figure 2 shows the effect of the wall angle (β) on the average Nusselt number for a channel aspect ratio of $A = 1.0$. As might be expected, increasing the magnitude of the angle (β) causes the average Nusselt number to decrease. However, it can be seen that positive values of β cause a greater reduction in the average Nusselt number than the same negative value of β. The greater reduction in heat transfer rate for $\beta > 0°$ occurs because the hot wall is tilted down and the cold wall is tilted up; this configuration is inherently more stable than the equivalent geometry with $\beta < 0°$ and produces weaker convective motion in the enclosure.

As shown in *Figure 3*, an attempt has been made to correlate the data. The variation of average Nusselt number minus the average Nusselt number for pure condiction ($\overline{Nu} - \overline{Nu}_{cond}$) has been plotted with the Rayleigh number (Ra^*) based on the actual height of the enclosure ($H' \cos \beta$). Although the correlation is far from perfect, the difference between the data from each wall angle is greatly reduced when compared with *Figure 1*. The curves for $\beta = 30°$, $60°$ are almost identical and are slightly lower than the $\beta = 0°$ data. The data for $\beta = -30°$, $-60°$ are slightly higher than the $\beta = 0°$ data.

Table 1 Comparison with the bench mark solution of De Vahl Davis and Jones[10] for a square enclosure ($A = 1$, $\beta = 0°$)

	De Vahl Davis and Jones[10]		Present Study	
Ra	$\overline{Nu}$	ψ_{max}	$\overline{Nu}$	ψ_{max}
10^3	1.118	−1.174	1.117	−1.174
10^4	2.243	−5.071	2.233	−5.117
10^5	4.519	−9.612	4.500	−10.09

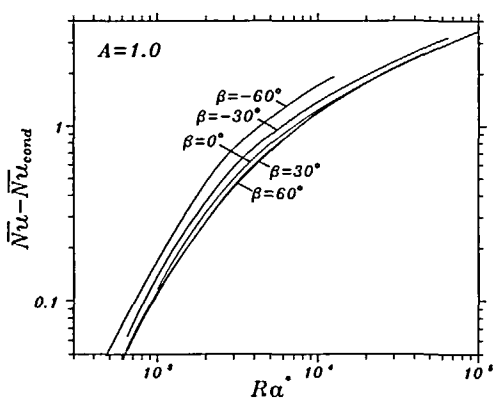

Figure 3 Variation of the average Nusselt number minus the pure conduction Nusselt number with Rayleigh number based on $H' \cos \beta$ for an aspect ratio $A = 1.0$

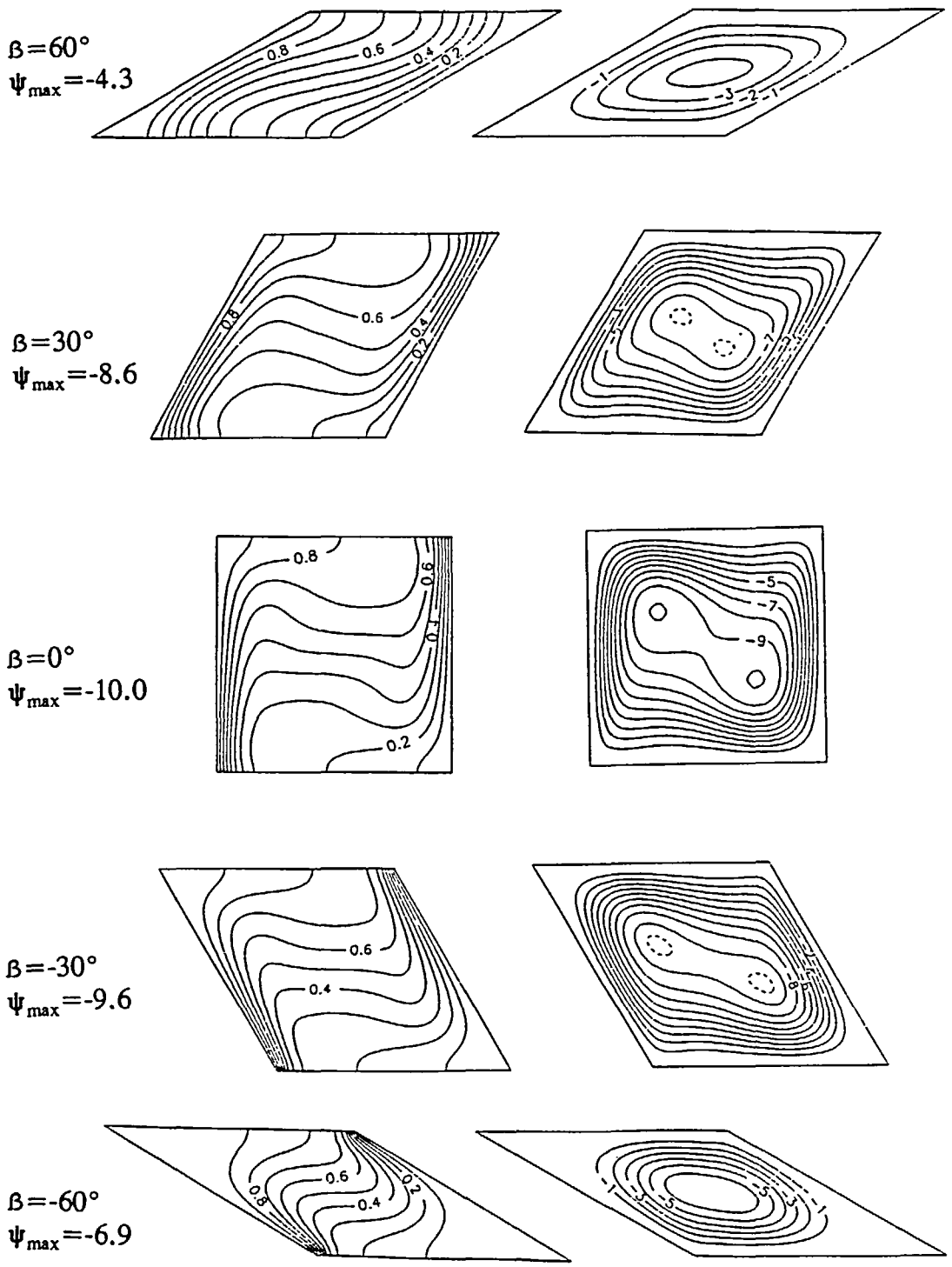

Figure 4 Streamline and isotherm contours for A = 1.0, Ra = 10^5, and $\beta = 0, \pm 30°, \pm 60°$.

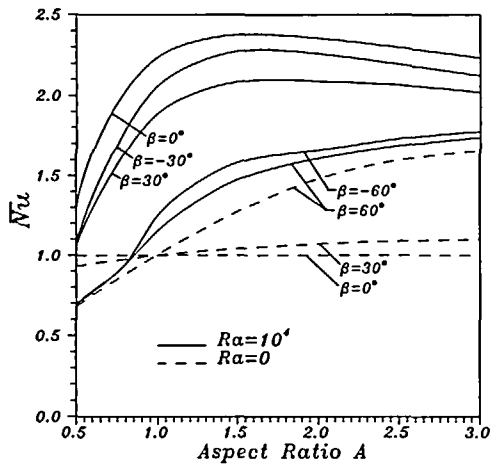

Figure 5 Variation of the average Nusselt number with aspect ratio for Rayleigh number of 10^4 and for wall angles $\beta = 0°, \pm 30°, \pm 60°$

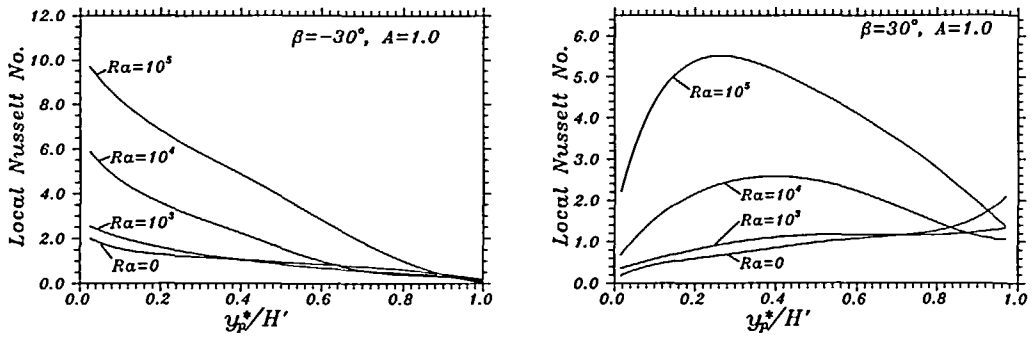

Figure 6 Local Nusselt number distributions for a wall angle (a) $\beta = -30°$ and (b) $\beta = 30°$ at several values of Rayleigh number ($A = 1.0$)

Streamline and isotherm contours at $Ra = 10^5$ showing the effect of the wall angle β are given in *Figure 4*. As mentioned previously, it can be seen from the streamline contours that positive values of β reduce the strength of the convective motion much more than the negative values of β. It is also evident that for $\beta = -60°$, that the convective cell is more elongated and penetrates deeper into the acute corners of the enclosure than for $\beta = 60°$. As a result, the temperature contours for $\beta = \pm 60°$ can be seen to be strikingly different.

Figure 5 shows the effect of aspect ratio (A) on the average Nusselt number for $Ra = 10^4$. To illustrate the relative contribution of conduction to the average Nusselt number, curves for $Ra = 0$ have also been shown. For $\beta = 0°, \pm 30°$ the maximum Nusselt number occurs near $A = 1.5$. For decreasing aspect ratios less than $A \approx 1.5$, the convective motion is reduced and the Nusselt number rapidly approaches the value for pure conduction. Above $A \approx 1.5$, although the convective cell strengthens with increasing aspect ratio, the increase in the convective heat transfer rate is smaller than the increase in the wall area. Hence, the average Nusselt number

decreases. In contrast, the Nusselt number for $\beta = \pm 60°$ increases continuously with increasing A. This is because the convective motion in the enclosure is weak for such large values of $|\beta|$; the conduction heat transfer rate, which increases with aspect ratio, dominates. However, it can be seen that the relative contribution of convection to the overall heat transfer rate peaks near $A = 1.5$ for $\beta = \pm 60°$.

Figures 6a and *6b* show the local Nusselt number distributions for $\beta = \pm 30°$ at various Rayleigh numbers. For $\beta = 30°$, the local Nusselt number decreases continuously toward the top of the hot wall. Also, it is particularly striking that heat transfer rate from the upper portion of the hot wall is almost zero, even at $Ra = 10^5$. In comparison, the local heat transfer distributions for $\beta = 30°$ are much more uniform. At $Ra = 10^4$ and $Ra = 10^5$ the distributions have maximum values part way up the hot wall that are much lower than the maximum local Nusselt numbers for $\beta = -30°$. Although the overall heat transfer rate is lower for positive values of β, for some applications the more uniform local heat transfer rate distribution may be preferred. It should also be noted that the solutions are diagonally symmetric, so these figures give the local Nusselt numbers for both the hot wall (bottom to top) and cold wall (top to bottom).

CONCLUSIONS

The results obtained in the present study show how the average Nusselt number for a parallelogram-shaped enclosure varies with the wall angle β. It has been found that positive values of β cause a greater reduction in the overall Nusselt number than the same negative value of β. Also, positive values of β produce a more uniform distribution of local heat transfer rates than negative β values.

ACKNOWLEDGEMENTS

This work was supported by the Natural Sciences and Engineering Research Council of Canada.

REFERENCES

1 Asako, Y. and Nakamura, H. Heat transfer in a parallelogram shaped enclosure, *Bull. JSME*, **25**, 1419–1427 (1982)
2 Yüncü, H. and Yamaç, S. Laminar natural convective heat transfer in an air-filled parallelogrammic cavity, *Int. Commun. Heat Mass Transfer*, **18**, 559–568 (1991)
3 Chung, K. C. and Trefethen, L. M. Natural convection in a vertical stack of inclined parallelogrammic cavities, *Int. J. Heat Mass Transfer*, **25**, 277–284 (1982)
4 Maekawa, T. and Tanasawa, I. Natural convection in parallelogrammic enclosures, *Proc. Seventh Heat Transfer Conf., München*, Vol. 2, pp. 227–232 (1982)
5 Seki, N., Fukusako, S. and Yamaguchi, A. An experimental study of free convective heat transfer in a parallelogrammic enclosure, *ASME J. Heat Transfer*, **105**, 433–439 (1983)
6 Yang, H. Q., Yang, K. T. and Lloyd, J. R. Buoyant flow calculations with non-orthogonal curvilinear co-ordinates for vertical and horizontal parallelepiped enclosures, *Int. J. Num. Meth. Eng.*, **25**, 331–345 (1988)
7 Lee, T. S. Laminar fluid convection and heat transfer in inclined trapezoidal chambers of low aspect ratio, *Fundamentals of Natural Convection*, ASME HTD Vol. 140, pp. 55–61 (1990)
8 Oosthuizen, P. H. and Paul, J. T. Free convection in a square cavity with a partially heated wall and a cooled top, *J. Thermophys.*, **5**, 583–588 (1991)
9 Oosthuizen, P. H. and Paul, J. T. Natural convective heat transfer across a cavity with elliptical ends, *Numerical Methods in Thermal Problems*, Pineridge Press, Swansea, Vol. 5, No. 1, pp. 356–367 (1987)
10 De Vahl Davis, G. and Jones, I. P. Natural convection in a square cavity: a comparison exercise, *Int. J. Num. Meth. Fluids*, **3**, 227–248 (1983)